catalysts

MDPI

Review

Enter the Tubes: Carbon Nanotube Endohedral Catalysis

Daniel Iglesias and Michele Melchionna *

Department of Chemical and Pharmaceutical Sciences, University of Trieste, Via L. Giorgieri 1, 34127 Trieste, Italy; d.iglesias.asperilla@gmail.com

* Correspondence: melchionnam@units.it

Received: 20 December 2018; Accepted: 17 January 2019; Published: 1 February 2019

Abstract: The unique morphological characteristics of carbon nanotubes (CNTs) present the intriguing opportunity of exploiting the inner cavity for carrying out chemical reactions. Such reactions are catalysed either by the individual tubes that function both as catalysts and nanoreactors or by additional catalytic species that are confined within the channel. Such confinement creates what is called "confinement effect", which can result in different catalytic features affecting activity, stability and selectivity. The review highlights the recent major advancements of catalysis conducted within the CNTs, starting from the synthesis of the catalytic composite, and discussing the most notable catalytic processes that have been reported in the last decade.

Keywords: carbon nanotubes; filling; endohedral; confinement; catalysis

1. Introduction

Since their discovery in 1991, there have been great expectations about the applicability of carbon nanotubes (CNTs) due to their unique properties [1]. Catalysis by CNT-based materials has enjoyed great popularity, and continues to be a very fruitful field of research [2], although the subsequent discovery of graphene (G) and its exceptional new features [3] has partly overshadowed the employment of CNTs in catalytic applications. It appears that G has centralized most of the attention of scientists in more recent years, and there has been a gradual shift towards the preparation of G-based catalysts. Despite its formidable properties, also useful in catalysis, there are some downsides in using G, above all its more difficult manipulation as compared to CNTs. This often compromises the homogeneity of the final hybrid or composite. Moreover, G may undergo much easier re-stacking of the individual sheets that deteriorate the catalytic properties. In comparison, separation of individual CNTs (particularly multi-wall CNTs, MWCNTs) is less demanding, especially if the CNTs are prefunctionalized [4]. In the wake of the curvature of the sp^2 framework in CNTs as compared to G, organic functionalization reaction may occur more favourably, as a result of the increased strain of the polyaromatic pattern [5]. Apart from considerations on the manipulation, functionalization and integration of CNTs into composites, there is one distinguishing aspect that may encourage use of CNTs in certain situations, and that is the possibility to exploit the internal space to confine other components. Internalization of different metal phases within the channels of CNTs has been reported to produce a variation of the behaviour of the incorporated entity, related to what has been termed *confinement effect* [6].

There are several dynamics taking place when foreign molecules are included within the CNTs. For example, the incorporation of water, alkanes and alkenes have been studied in detail both experimentally and theoretically and compared to the adsorption on the outer walls of the CNTs [7]. These molecules can adsorb with higher binding energies as the Van der Waals forces are enhanced due to restricted space and the favourable curvature of the tubes (as opposed to the exterior where

the curvature stays away from the adsorbate) [8]. The stability of certain metal crystal phases can also be considerably affected, such as the case of face-centred cubic (*fcc*) γ-Fe nanoparticles, which are stable under normal conditions in the approximate range of 1100–1600 °C, but that retain their crystal structure at room temperature when confined in CNTs [9]. On the other hand, the crystal structure of the enclosed species undergoes distortion in some cases [10]. Milestones works on the inclusion of fullerenes has indicated that the molecule has a low barrier of motion despite the increased Van der Waals forces [11]. Indeed, a variety of fascinating properties arise upon endohedral confinement of foreign species within the CNTs channels, and the possibility to carry out specific reactions between molecule inside the aromatic cylindrical framework was envisioned some time ago, tailored by CNT definite parameters such as diameter, affinity towards specific molecules or chirality of the CNT. The opportunity of catalyst confinement goes beyond the exploitation of the CNTs as nanoreactor [12], given the change of properties of the confined phase and the potential electronic participation of the interior walls of the CNTs into the catalysis. Still, the mere utilization of the nano-constrained channel of the CNTs, with no added extra catalyst, can lead to dramatic changes of the reactivity pathways of several chemical transformations.

This review does not aim at reporting all the physical characteristics change upon endohedral confinement within CNTs, but it rather focuses on the catalytic aspects as reported in the last decade. Indeed, it has been proven that a complete switch in terms of selectivity or activity can be effected by relocating the metal active phase from the outside to the inner space of the tubes, as well as other more general advantages can be achieved. The paper focuses on more recent contributions, and it will inevitably overlook some of the earlier work, which however has been instrumental to the further development of materials. Several outstanding reports on catalytic reactions by filled CNTs such as the NH_3 decomposition by Fe-Co@CNT [13] or the ethanol production by Rh@CNTs [14] surely paved the way to the broader adoption of this type of catalysts, but they will not be included as the goal is to provide an update of work in this field. The review is divided in two parts; the first outlines the general pathways for the synthesis of endohedrally filled CNTs, and the second describes the most prominent examples of catalysis by these fascinating materials in recent years.

2. Synthetic Aspects

There are different synthetic approaches to accessing the internal cavity of CNTs. As prepared CNTs are typically tip-closed, meaning the ends of the CNTs are blocked for the insertion of foreign molecules or chemical species. Therefore, ex situ approaches require a tip-opening step before the endohedral functionalization. This is commonly done by thermal annealing or by acid treatment (i.e., H_2SO_4/HNO_3 or HNO_3). A pioneering work was reported by Tsang et al., who could insert several metal oxides by wet techniques after a tip opening by refluxing in concentrated HNO_3 [15]. It is commonly accepted that one of the principle that drives the metal oxide (or other species) within the interior of the tube is based on exploiting capillary forces, upon evaporation of the solvent in which the entering species is dissolved, although entrance of the endohedral component may begin before, particularly if refluxing is performed. Talyzin et al. carried out two thermal annealing treatments under air at 380 °C, separated by an acid washing step (with HCl) that served to remove any metallic particles inherent to single-walled CNTs (SWCNTs), obtaining open, void SWCNTs ready to be filled by aromatic molecules [16]. On the other hand, the preparation of filled CNTs by in situ methods exploits CNTs synthesis to produce filled tubes in one step. For instance, very recently some of us have reported the synthesis of MWCNTs filled with Fe on its α-, β- and carbide form, where the iron functions as a metal centre for the developing of the tubular carbon structure, remaining partly entrapped within [17]. This and other analogous protocols are carried out at high temperatures (i.e., 900 °C) with a rigorous control of reaction conditions such as carbon precursor, flow rate, time of residence at the set temperature and location of the metal catalyst within the furnace. Small variations of the conditions can lead to a dramatic difference in morphology. Because the required catalyst for the

growth of nanotubes are metal complexes, the in situ approaches are limited to the encapsulation of metal nanoparticles.

Nowadays, the vast majority of reports use CNTs prepared by chemical vapour deposition (cvd) in the presence of metal catalysts following a number of operative conditions. This gives rise to materials of various thicknesses, lengths, number of walls (single-, double-, triple- or multi-walled CNTs), levels of defectiveness or morphology. All these aspects may have positive or negative effects on the further endohedral modification with additional entities. Sengupta and Jacob performed a systematic study of the effect of Ni and Fe as metal catalysts. The data suggests that in both cases MWCNTs develop through a tip-growing mechanism [18]. The observation of both samples by HR-TEM showed that Fe-containing CNTs are straight hollow tubes with elongated Fe particles inside, while CNTs synthesize with Ni present a bamboo-like structure with lower crystallinity according to the XRD analysis (Figure 1). Thus, endohedral functionalization prepared with Ni would be hampered by the presence of internal walls within the tube. It has been described that internal Ni impurities can be removed when heated in the presence of melamine at elevated temperatures [19]. The process reactivates the particles inducing their leaching from the carbon shell. The expelled metal impurities act as active sites for the water oxidation reaction with high turnover frequency.

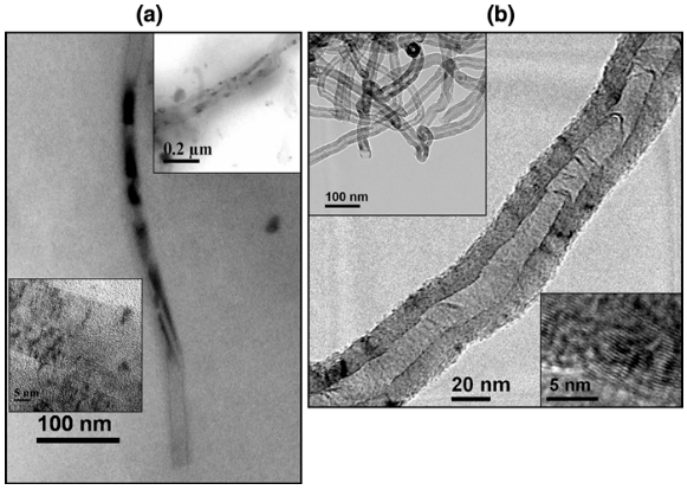

Figure 1. High-resolution transmission electron microscopy (HR-TEM) images of straight (**a**) and bamboo-like (**b**) MWCNTs. Reprinted with permission from reference [18]. Copyright Springer Nature.

The influence of the level of defectiveness is not that obvious. Several processes and equilibria may happen simultaneously during CNT endohedral functionalization. During this energy-balanced competition, the presence of functional groups (i.e., oxygen containing functional groups) would boost the interaction with the second component, tipping the balance (equilibria) towards the adsorption in the outer walls. In fact, the functionalization of CNTs is very often the first step in the synthesis of CNTs hybrids, in which the outer walls of the tubes is covered with a second component [4]. Differently, endohedral CNTs endohedral functionalization benefits from the absence of interaction between the outer CNTs surface and the second component. Baaziz et al. stressed the advantages of CNTs repristination [20]. After an initial acid treatment to wash out any remaining metal, CNTs were annealed at high temperatures (i.e., up to 900 °C) to remove the residual functional groups. X-ray photoelectron spectroscopy (XPS) analysis showed that oxygen-containing groups are completely eliminated at 650 °C, yet other kinds of defect might still be present. Comparison of as-received and pretreated samples clearly shows the advantages of CNTs restoration. The untreated sample presented practically no $Fe_{3-x}O_4$ encapsulation. On the other hand, the annealed sample exhibited 95% encapsulation with very few NPs in the outer surface as unambiguously confirmed by TEM tomography inspection (Figure 2). This approach has been proved to be successful for other types of NPs [21].

Another successful strategy involves the post-modification of the oxygen-containing functional groups introduced through different oxidative protocols. This modification aims also at reducing the affinity between CNTs and NPs, thus promoting encapsulation. Castillejos et al. oxidized MWCNTs and then linked long alkylic chains through amide coupling reaction. The non-polar chains cover MWCNTs and prevent the π-π interaction with NPs stabilizer (i.e., 4-(3-phenylpropyl)pyridine), which guides NPs towards the inner cavity of MWCNTs [22].

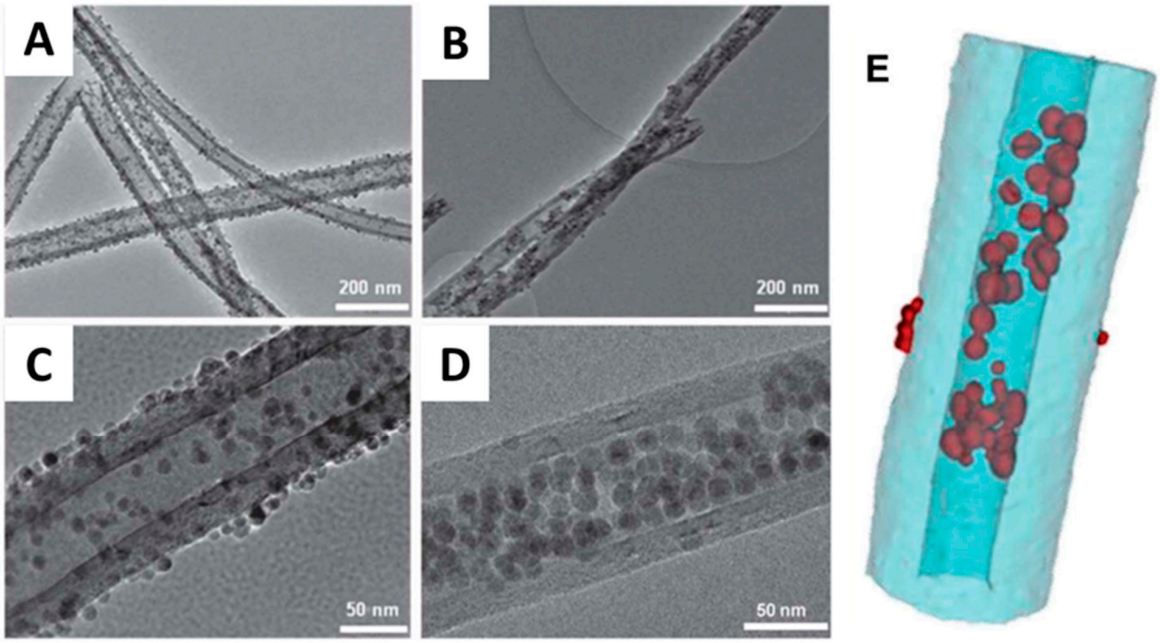

Figure 2. TEM images at different magnifications of $Fe_{3-x}O_4$ localized inside and outside MWCNTs (**A**–**D**) and tomography reconstruction of $Fe_{3-x}O_4$ nanoparticles inside MWCNTs (**E**). Adapted with permissions from reference [19]. Copyright Royal Society of Chemistry.

The thickness and length of CNTs are factors whose effect in the endohedral functionalization seems clearer. Ersen et al. used electron tomography to characterize hybrid materials composed of CNTs and Pd nanoparticles [23]. By this means, the authors managed to locate more than 50% of Pd nanoparticles inside 30-nm-thick MWCNTs. Contrarily, the filling efficiency went to almost 0% when 15-nm-thick MWCNTs were used. However, a more recent report shows that the encapsulation of nanoparticles in thin SWCNTs is indeed possible. The situation is completely different when the internalized agents are discrete organic molecules or inorganic salts both molten or diluted. The possibility of introducing ferrocene within 1.4-nm-thick SWCNTs prepared by arc discharge was already reported in 2005 [24]. Accessing of discrete molecules within thin SWCNTs is indeed possible and has been reported in many different works. In a recent example, Nieto et al. adapted a previously reported protocol [25,26] to encapsulate viologen derivatives in 1.6–2.2-nm-thick metallic SWCNTs causing a band-gap opening of the nanomaterials [27]. Following a completely different approach, Kierkowicz et al. prepared SWCNTs filled with $LuCl_3$ whose radioactive isotope ^{177} Lu is largely used in medicine [28]. To do so and in line with most recent reports, SWCNTs were purified i.e., (i) oxidation; (ii) acid treatment to remove the catalyst; and (iii) annealing to restore the graphitic nature) and then grinded in the presence of the salts. This mixture was sealed under vacuum before thermal treatment above $LuCl_3$ melting point for 12 h. In this way, the internalization of the salts comes together with the tip closing of SWCNTs, which is particularly interesting to protect against possible leaching.

Due to the special feature of ^{177} Lu (i.e., short half-life time radioactivity) the authors brought to scene the importance of the purification of this kind of materials, where necessarily significant fractions of metal species may depose on the outer walls of the CNTs, making complex a clear understanding of the composite properties. After trying different methods of purification combining sonication, filtration,

dialysis and Soxhlet extraction, best results were obtained when dialysis was coupled to a Soxhlet apparatus. In other works, sublimation, multiple centrifuge washings or repetitive sonication/filtration cycles are carried out to eliminate the large excess of non-encapsulated molecules [26]. When these repetitive treatments are done in acid media, a large portion of metal nanoparticles bound to the outer walls of CNTs can be removed [29].

For catalytic applications, it becomes sometimes necessary to post-functionalize the filled CNTs by standard organic reactions. This is done for example to equip the outer part of the tubes with polar groups able to enhance the dispersibility of the materials in aqueous or polar solvents (for liquid phase catalytic applications), or to be able to anchor secondary catalytic species. Derivatization leading to tip-opening or graphitic wall piercing must be avoided to retain the endohedral component. Two illustrative examples have been recently reported. D'Accolti et al. exploited the reactivity of dioxiranes to functionalized SWCNTs filled with metal halides, which generate epoxide groups on the surface of the nanostructures [30]. Subsequently, the epoxide were reacted with an excess of 1,6-hexamethylendiamine obtaining closed, filled, functionalized SWCNTs with amine pendant groups and moderate increase of the dispersibility in water. Marega et al. funtionalized Fe-filled MWCNTs for potential application in cancer treatment (Figure 3) [31]. Following the diazocoupling protocol [32], protected amino groups were linked to the outer walls of MWCNTs. Interestingly, the deprotection carried out in HCl (4 M): dioxane for 24 h did not significantly alter the amount of encapsulated Fe. Eventually, the free-amino groups were covalently linked to Cetuximab or Bovine Serum Albumin for the biological application.

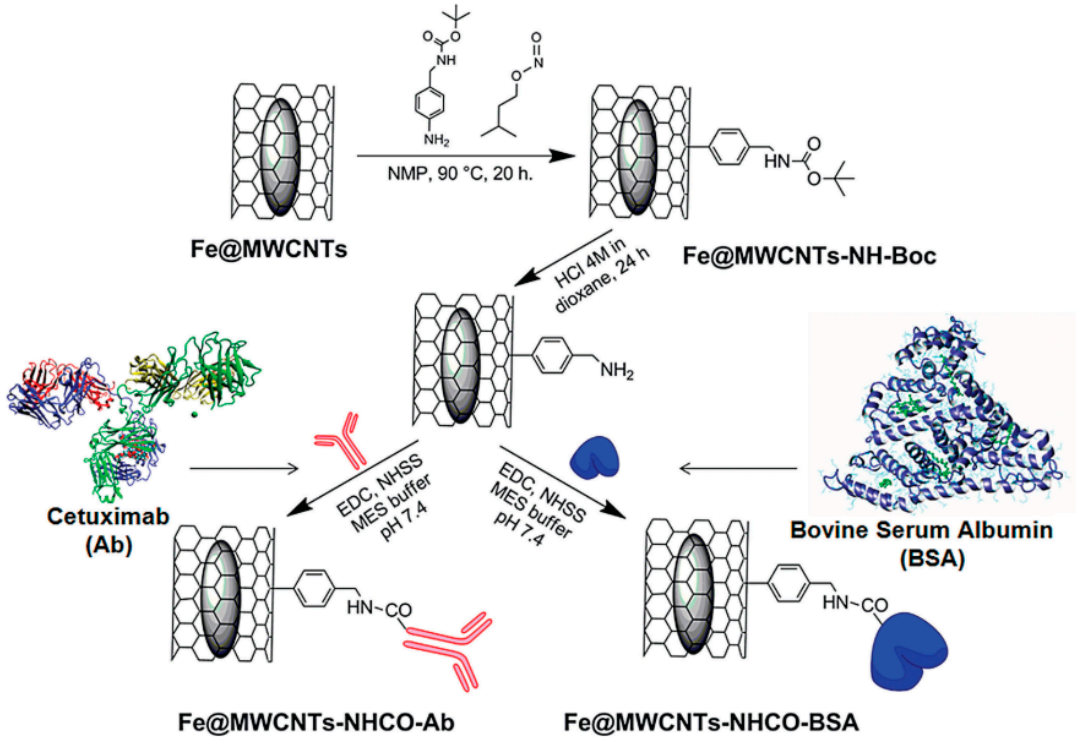

Figure 3. Organic functionalization of Fe-e filled MWCNTs. Reprinted with permissions from reference [30]. Copyright Wiley and Sons.

The fast development of nanotechnology has been partly stimulated by the very encouraging results and the advances in the characterization techniques. In line, the complexity and performance of the frontier materials is increasing. In a very elegant example, Chen et al. synthesized a hybrid material composed of reduced graphene oxide (RGO) and N-doped CNTs with encapsulated Co NPs for the electrocatalytic production of hydrogen (Figure 4) [33]. The synthesis starts with the deposition of Zn^{2+} rGO basal plane exploiting the oxygen containing functional groups. The addition

of 2-methylimidazole to that complex triggered the formation of ZIF-8 particles in situ on top of RGO. The formed ZIF-8 acted as growing points for ZIF-67 water, resulting in a 2D material covered by ZIF-8 and ZIF-67 with a core-shell structure. Eventually the annealing of this material under argon at high temperatures caused the formation of Co NPs and the growing of N-doped CNTs from graphene.

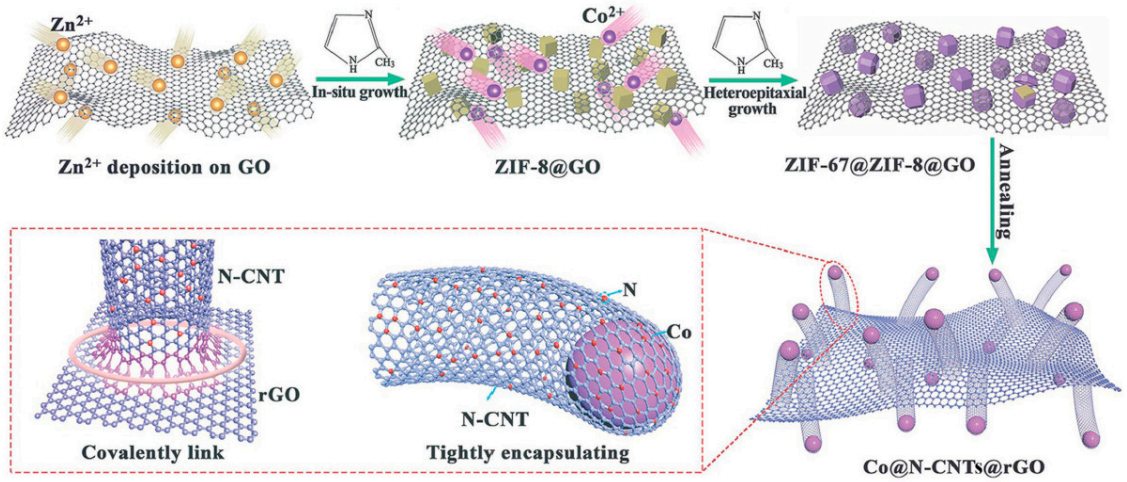

Figure 4. Multistep synthesis of the hierarchical material composed of rGO and N-doped CNTs with Co NPs encapsulated. Reprinted with permissions from reference [32]. Copyright Wiley and sons.

The complexity of the synthetic procedure for accessing filled CNTs has reached high levels, inspired by the structure-function of the finale materials, where synergy of phases is often sought to boost performance in the specific application.

3. Catalysis

The endohedral functionalization of CNTs leads to the so-called *confinement effect*. In 2011, Pan and Bao revised the topic identifying several aspects that may contribute to this effect [6]: (i) different electronic interactions when metal nanoparticles are inside or outside CNTs; (ii) a variation in the molecules classical arrangement due to the limited space, for instance, a water molecule adopted an unusual cyclic configuration [34]; (iii) reactant enrichment in the interior walls; and (iv) transport resistance along the CNT longitudinal axis. All these aspects are directly related to the effect of internalization and catalysis when CNTs are considered as nanoreactors, i.e., the reaction under study happens inside the tubes and the product(s) leave the tube eventually. However, there are other examples where endohedral functionalization is important, yet CNTs are not exclusively considered as nanoreactors. Hereafter, we will describe some of the most recent examples of filled-CNTs contributed to the catalytic process also by other means. Several modes of reactions can be identified and we have attempted to graphically describe them in Figure 5.

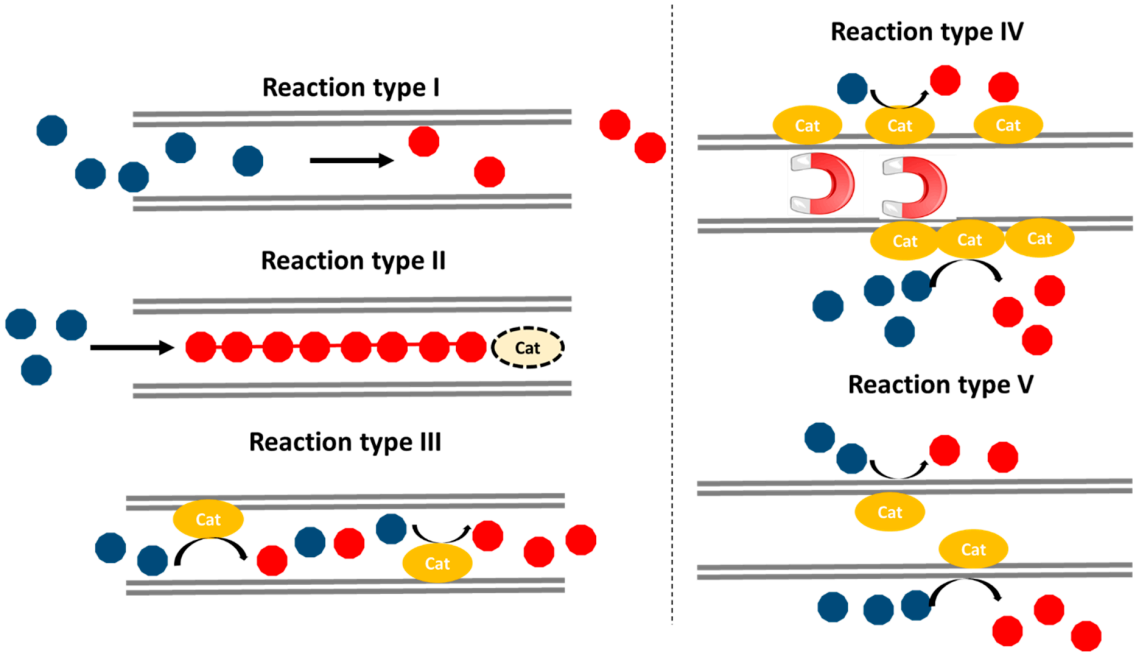

Figure 5. Different type of reactions involving endohedral CNTs. The dotted line around the catalyst in reaction type II indicates that the reactions may occur with or without catalyst. Blue balls: reagents; red balls: final product.

4. Nanoreactors–Reactions Type I and II

Classically, a reactor is considered as the container were a reaction takes place. In this context, the newly coined term 'nanoreactor' restricts the dimensions of the place where the reaction occurs. Therefore, apart from the classical reaction conditions (i.e., temperature, reactants concentration, stirring speed, etc.) new aspects such as CNTs internal diameter comes into play. In the literature, many kinds of reactions have been described to take place within CNTs without the aid of additional catalysts, thus it must be deduced that the catalytic effects derive simply by the nanoconfinement. The list covers all sorts of reactions including photocatalytic and electrocatalytic transformations, cycloadditions, halogenations, hydrosylilations, hydrogenations, oxidations, a range of syngas conversions, etc. [35]. All these reactions can be classified in three main groups: (i) the reactants enter the CNTs, undergo a chemical reaction and leave; (ii) the reactants enter the CNTs, suffer a chemical modification and remain encapsulated; and (iii) the reactants enter the CNTs, undergo a chemical reaction driven by an endohedral catalyst and leave.

The differences between the first two types of reaction lay in the nature of the final product(s). In many reactions, the internally formed molecules or materials are difficult to collect due to the large Van der Waals forces. Inherently, their study requires very sophisticated characterization techniques (i.e., advanced microscopy). Differently, largely available techniques such as NMR or IR could be apply in the processes were the product leaves the nanomaterial. Surprisingly, while there are many examples of reactions where the products remain encapsulated inside the CNTs nanoreactor, the literature is still scarce on preparative reactions for accessing useful organic products that can be extracted from within the CNTs. The first example of this kind was reported in 2013 by Miners et al. [36]. In this work, the authors studied the halogenation of N-phenylacetamide with bypiridiniumdichlorobromate. This reaction yields a mixture of regioisomers with 68% of *para*- and 32% of *ortho*-substitution (Figure 6a). Outstandingly, the proportion of the *para*-isomer increased up to 97% when the reaction takes place within CNTs. The molten starting material was encapsulated inside SWCNTs at 120 °C at reduced pressure. This protocol led to a non-homogeneous mixture of encapsulated and non-encapsulated material that turn out to be very useful to study the effect of confinement. The adsorbed N-phenylacetamide was gradually removed by distillation.

This permitted to perform the halogenation at N-phenylacetamide: SWCNTs ratio ranging from ~2100 (i.e., mainly nonencapsulated) to ~9% (i.e., only encapsulated) observing a significant effect of confinement. A control experiment with close SWCNT confirmed the role of CNTs as nanoreactors. The experiment with SWCNTs of different dimensions confirmed that subtle variations in CNT diameter (i.e., from 6.9 to 9.6 Å) are crucial to get the desired effect. The in silico study of this reaction led to the hypothesis that the non-covalent interactions within CNTs is the main contributing factor to explain the regioselectivity and the kinetics of the reaction [37].

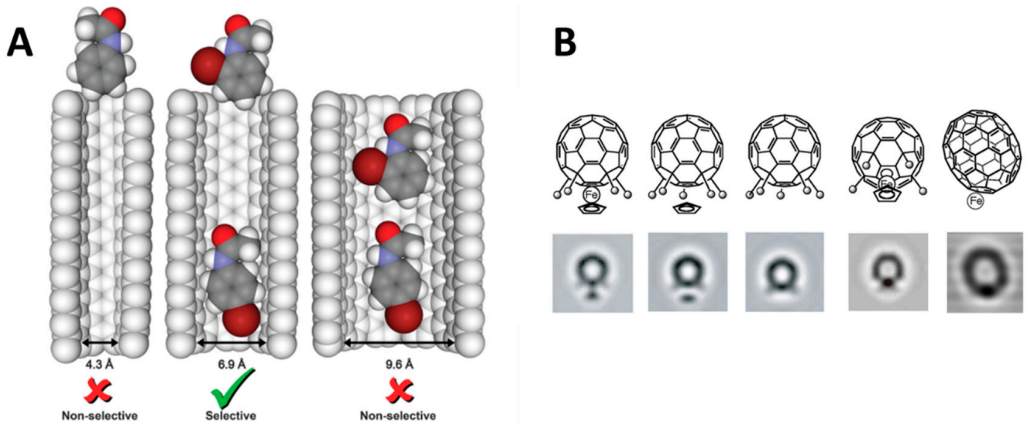

Figure 6. Comparison of Van der Waals diameter of SWCNTs with different widths and its compartison with N-phenylacetamide (**A**); reprinted with permissions from reference [35]. Copyright Royal Society of Chemistry. Molecular model and TEM simulation of a bucky metallocene reorganizing to form a C_{70} fullerene (**B**). Adapted with permission from reference [37]. Copyright (2011) American Chemical Society.

The following examples are dedicated to the second type—reactions where the process occurs inside CNTs and the product remains encapsulated. Somehow, this type of reactions may resemble a strategy to prepare endohedrally modified CNTs. However, here we put the focus on the effect of confinement to explain a chemical transformation. For instance, in the work by Talyzin et al., coronene and perylene, respectively, were transformed into graphene nanoribbons (GNRs). Previous reports showed that coronene fusion require at least 530 °C [38], while inside SWCNTs the process occurs already at 450 °C. Therefore, confinement results in a positive catalytic effect lowering the onset temperatures, which led to the formation of oligomers and carbon particles of challenging purification and characterization. TEM showed GNRs of different conformations (e.g., straight or helical) and Raman characterization revealed differences between coronene-GNRs and perylene-GNRs. Notably, SWCNTs were almost quantitatively filled with GNRs. Apart from the fundamental implications, the importance of this work lays on the macroscopic synthesis that allows further development of such materials. Similar materials have been prepared by rather different approaches. This is the case of encapsulated GNRs reported by Khlobystov and co-workers with proved expertise in the topic. In the first work, the team reported the synthesis of sulphur-terminated GNRs after long exposure to an electron beam (i.e., in situ in the TEM instrument) [39]. Initially, an ad hoc $ScN_3@C_{80}$ functionalized with N, O, H and S was prepared, in order to incorporate atoms able to terminate the edges of GNRs. Upon e-beam exposure, the guest fullerene decomposed into S-terminated GNRs. They realised that such synthetic efforts were not required since the 1D material could be also prepared when tetrathiafulvalene with or without fullerene was bombarded with electrons. This suggests that the mechanism occurs through the growing of small C_2 fragments. In this case, SWCNTs act both as containers (i.e., avoiding the fast diffusion of the small fragments) and as templates. Further investigations of this process highlighted the importance of the templating effect [40]. SWCNTs smaller than 1 nm yielded just atomic chains and inside SWCNTs wider than 2 nm, amorphous materials and nano-onions were formed.

In the same line, several examples of reactions involving fullerenes encapsulated in CNTs have been reported. These reactions are nanometrically localized and are not scalable but may be very useful in catalysis and in chemical education, as highlighted by Nakamura et al. [41]. In this example, the C-C rearrangement of two different bucky-metallocenes made of Fe and Ru, respectively, was studied under TEM inspection (Figure 6b). The tight confinement within the 'peapods' prevented the metal aggregation into clusters, consenting the study of a single-metal catalysis process. The results showed that group 8 metals catalyse these C-C rearrangements likely towards C_{70} cages, while other bucky-metallocenes with La or Er do not. The same team studied also dimerization reactions under e-beam irradiation of classical C_{60} within CNTs [42]. The fusion occurs in two steps. First, a reversible dimerization takes place presumably through a [2+2] mechanism. Second, the dimer evolves towards an unusual peanut-like structure. SWCNTs provide a unique environment where C_{60} movement is restricted to one dimension.

Apart from nanocarbons, several other species can be formed inside the CNTs, including organic and inorganic polymers, inorganic nanocrystals or single layered materials. In most cases, the confinement effect has the role of templating the growing of linear structures. Encapsulated polyadamantane represents a nice bridge between nanocarbons and polymers [43]. This kind of polymers can be considered as linear nanodiamonds. The polymerization did not occur on purified CNTs, calling for a fundamental role of residual metal catalyst. The authors suggested a step-wise mechanism of the whole process. The monomer is adsorbed on the outer aromatic surface. Then, during the diffusion towards the internal cavity, they interact with Fe particles forming the biradical species that polymerize inside CNTs (Figure 7a). The synthesis depends strongly on CNT inner space, with 1 nm width CNTs being optimal for the formation of the chains. In wider cavities, monomers/oligomers can rotate freely, leading to the formation of amorphous particles. Similar templating effects have recently been observed for the formation of polythiophenes [44]. Very thin CNTs do not provide the required space. As the internal diameter increases, one, two or three layers of polymers are stacked in 1.0, 1.5 or 1.7 nm, respectively. Larger diameters led to the formation of non-linear structures (Figure 7b). This type of reaction may also occur in the presence of a catalyst. This would be the case of the isoprene polymerization reported by Li et al. [45]. Fe NPs were decorated with iminopyridine and their catalytic activity was studied and contrasted with the catalytic activity by Fe NPs inside CNTs. Magnetic characterization showed that the polymerization is less efficient inside CNTs. It is suggested that diffusion and the interaction between CNTs and the aromatic ligand hamper the process inside CNTs.

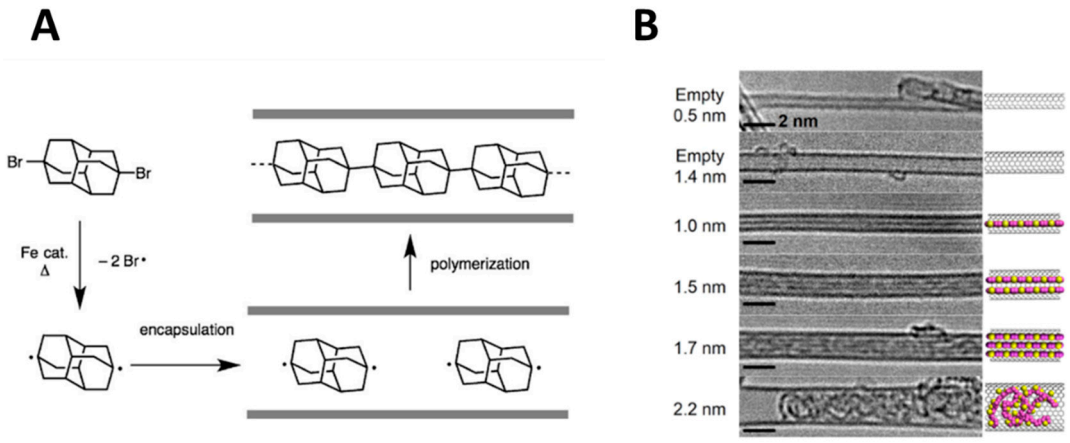

Figure 7. Proposed mechanism for the formation of linear polyadamantane inside SWCNTs (**A**); reprinted with permissions from reference [42]. Copyright Wiley and Sons. HR-TEM images and models showing the influence of CNTs diameter on the encapsulation of polythiophenes (**B**). Adapted with permission from reference [43]. Creative Commons Attribution 4.0 International License 2018.

Recent works have also described the encapsulation of inorganic materials with potential use in several technological applications. For instance, Cabana et al. reported the synthesis of single-layered

materials within CNTs for the first time (Figure 8) [46]. Particularly, PbI_2 single-walled nanotubes were templated within MWCNTs. Other reports had shown the formation of PbI_2 multi-walled nanotubes exploiting other templating agents [47,48], yet the formation of single layered materials is so far exclusive to MWCNTs. Statistical TEM analysis concluded that at least 4 nm diameter is required for nanotube formation, while concomitant nanorods showed no threshold. This is due to the decrease of Van der Waals and the increase of tubular tension as the diameter is reduced. This threshold can decrease up to 3 nm for BiI_3 nanotubes [49].

Although very powerful, the effect of CNTs is not limited to templating. Toxic, water-soluble $HgCl_2$ was transformed into Hg_2Cl_2 within CNTs, with the latter contributing to the transformation via electron transfer pathways, donating electron density [50]. Functional groups pendant to carbons have also exploited for the same redox reaction [51], with the consequent oxidation of the carbon material. Diversely, SWCNTs suffered any major modification when the redox reactions occurred inside their cavity, calling for a catalytic effect. A charge-transfer from SWCNTs to the inorganic salt was identified also on the basis of computational modelling. The excess of charge is used for the redox process and then transferred back to SWCNTs.

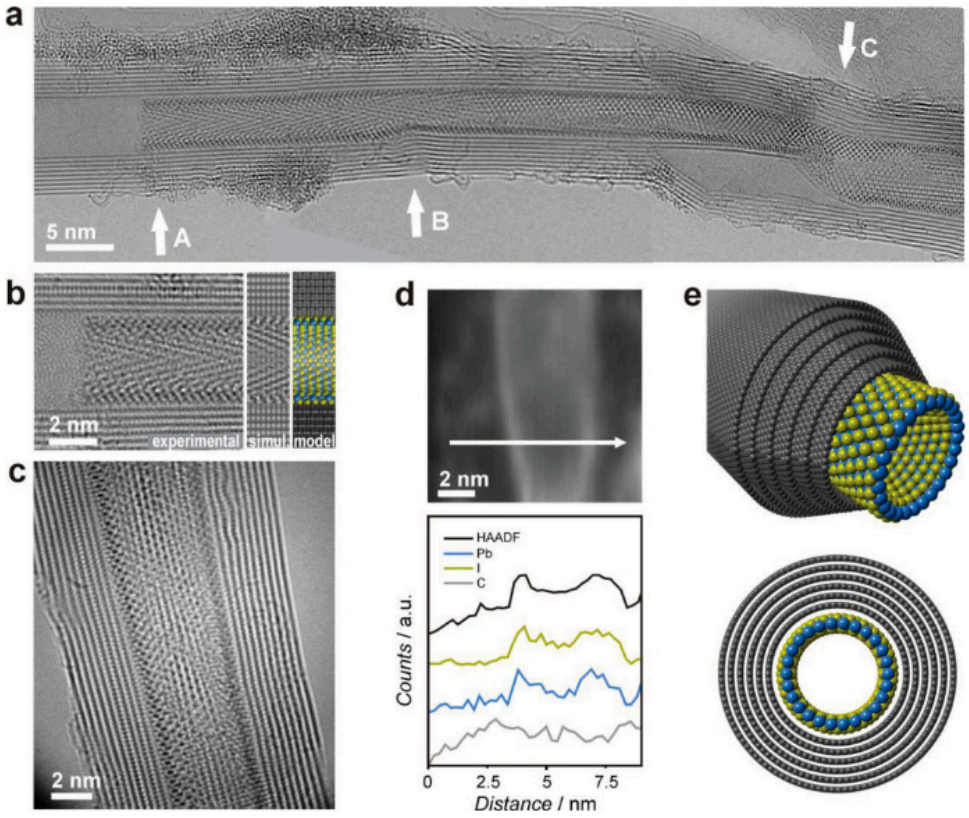

Figure 8. HR-TEM, aberration corrected image of PbI_2 NTs encapsulated in MWCNTs (**a**,**c**); enlargement of A and its comparison with the TEM simulation and model (**b**); Scanning TEM-energy dispersive spectroscopy (STEM-EDS) of PBI_2 NTs (**d**) and; schematic representation of the hybrid (grey: carbon, green: iodine and blue: lead) (**e**). Reprinted with permissions from reference [45]. Copyright Wiley and sons.

5. Reactions Type III

This part combines advantages of heterogeneous catalysis using metal supported nanoparticles (e.g., tuneable size and composition, recyclability, etc.) with confinement effect. The effect of confinement is not always positive, which requires 'case by case' investigation for any given reaction. For instance, Au NPs of different sizes (i.e., 18 or 2–7 nm) encapsulated inside MWCNTs exhibited low activity towards CO oxidation under hydrogen-rich stream [52]. On the other hand, the oxidation

of cyclohexane catalysed by 3–5 nm Au NPs was four times more performant when Au NPs were encapsulated and not just exohedrally deposited [53].

Studying the confinement effect is rather challenging. A widespread strategy to study consists in the preparation of a reference material with NPs deposited on the outer surfaces of CNTs. Cui et al. prepared MWCNT filled (and/or covered) with CdS NPs for photoactive dye degradation in aqueous media under visible light irradiation [54]. Both materials showed higher activity than bare CdS NPs. The confinement effect was less important for the actual catalytic activity by the composite catalysts as endohedral NPs displayed lower activity than exohedrally deposited NPs. However, it appeared to be essential for the recyclability of the catalyst. External NPs lost their activity drastically already after one catalytic test, while confined NPs activity was stable within the studied range (i.e., up to four cycles). This shows another positive consequence of confinement, which helps reducing the operational cost of the final catalyst. The authors explained that increase of activity (compared to CdS NPs) by the tight heterojunction between CdS NPs and CNTs that boosts the charge separation. Regarding the photostability, it was proposed that the higher concentration of methylene blue inside CNTs avoids CdS decomposition, as the produced holes are readily consumed by the dye (Figure 9).

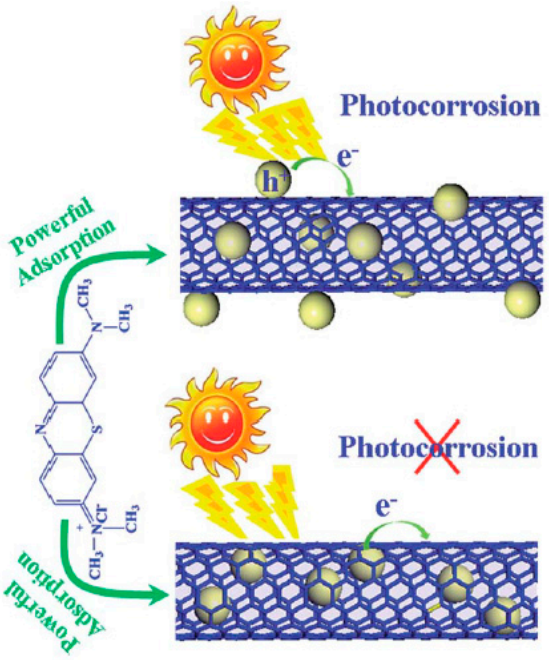

Figure 9. Schematic representation of the hybrids materials made of adsorbed (up) and encapsulated (down) CdS NPs on MWCNTs and the corresponding catalytic processes. Reprinted with permission from reference [53]. Copyright Royal Society of Chemistry.

Combination of endohedral semiconductors with CNTs for photocatalytic applications is an interesting topic that has attracted attention as well as criticism. It is suggested that confining semiconductors inside CNTs would decrease their ability to absorb light, in relation to the shielding of the carbon layers. However, it has been reported the enhanced photocatalytic degradation of methylene blue (MB) under visible light by a composite consisting of TiO_2 confined inside CNTs than the corresponding composite where TiO_2 was attached externally to the CNTs. The increased catalytic activity of the former (prepared exploiting wet methods and capillary forces) was explained in terms of a modification of the electronic structure of the endohedral TiO_2, with enhanced formation of oxygen vacancies and correspondingly of Ti^{3+} centres [55]. The resistance to sintering of inner nanoparticles has been often observed for various types of reactions. For example, the Suzuki coupling by Pd@CNTs was reported to have a high recyclability as a consequence of the pronounced sinter-resistance under the catalytic conditions. The synthesis of the Pd@CNTs catalyst relies on a fascinating approach, where

the Pd NPs are first deposited on ZnO tubes and then covered with the carbon layer. Removal of the inner ZnO by acid washing leaves Pd NPs intimately attached to the inner cavity of the CNTs, although the properties of the CNTs prepared via this method are presumably different from CNTs made from standard protocols (Figure 10) [56].

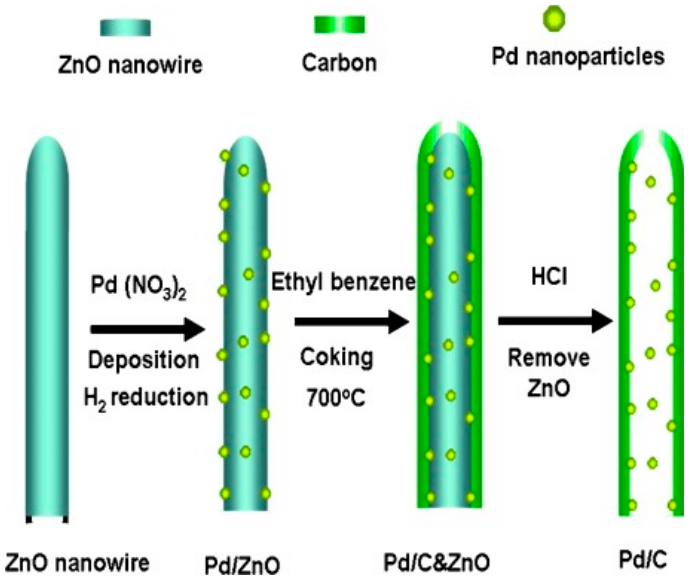

Figure 10. Scheme of the synthesis of Pd/C nanocomposites with Pd NPs within the CNTs. Reprinted with permissions from reference [55]. Copyright Wiley and Sons.

The promising results in this area have encouraged investigations towards reactions with major industrial applications, such as the Fischer-Tropsch (FT) or ammonia syntheses. In the FT reaction, H_2 reacts with CO in the presence of metal catalyst to form mixtures of hydrocarbons. Chen et al. exploited the confinement effect in the FT reaction. CNTs with encapsulated Fe_2O_3 displayed up to 1.4 times higher activity than the material with NPs in the outer surface [57]. Besides, the encapsulated catalyst suffered only minor modification after up to 200 h of reaction, while the external particles tend to agglomerate into bigger particles. Moreover, the selectivity towards long-chain hydrocarbons (i.e., five or more C atoms) was also higher when the reaction occurred inside CNTs. The higher selectivity is a consequence of confinement: the limited space within the nanoreactor hinders the diffusion of products favouring the hydrocarbon chain growth. In line with the higher performance, the generation of carbides, the most active phase, was higher in endohedral NPs. The inner part of CNTs is electron deficient due to the curvature. Then, the NPs-CNTs interaction between the two areas (outer and inner) is different. Inner part are more destabilized and consequently more prompt to form active species. The electron deficiency of the inner face of CNTs explained the observed lower activity of Ru NPs encapsulated in MWCNTs in the synthesis of ammonia, and combined experimental and in silico analyses aided to formulate solid hypotheses [58]. In this case, endohedral Ru NPs were less active than adsorbed NPs. It is known that electron rich catalysts accelerate the reaction as N_2 dissociates in the rate determining step through an electrophilic process. This example reinforced that confinement is not always positive for catalytic purposes. The reversed reaction, the decomposition of ammonia, was also explored by Ru/CNTs catalysts, comparing Ru "in" and Ru "out", and correlated also with the size of the NPs, resulting in an interesting and unexpected enhancement of activity in parallel to the increase of size, for both inner and outer NPs [59].

Enzyme-mimicking, more specifically peroxidase-like activity, by filled CNTs was also reported where Prussian Blue (PB) was introduced inside CNTs via a facile wet filling procedure, removing any outer ad-mixture with centrifugation. The material turned out to be a promising catalyst for application in biosensing (H_2O_2 and glucose) [60]. The same authors also used a similar catalyst for the electrochemical reduction of H_2O_2, proving that the expected low mass transfer inside the CNTs

channel does not pose a limitation, while leaving outer surface of the CNTs available is an asset for adsorbing other molecules, such as 4-(1-pyrenyl) butyric acid, able to anchor glucose oxidase or lactate oxidase for biosensing applications (Figure 11) [61].

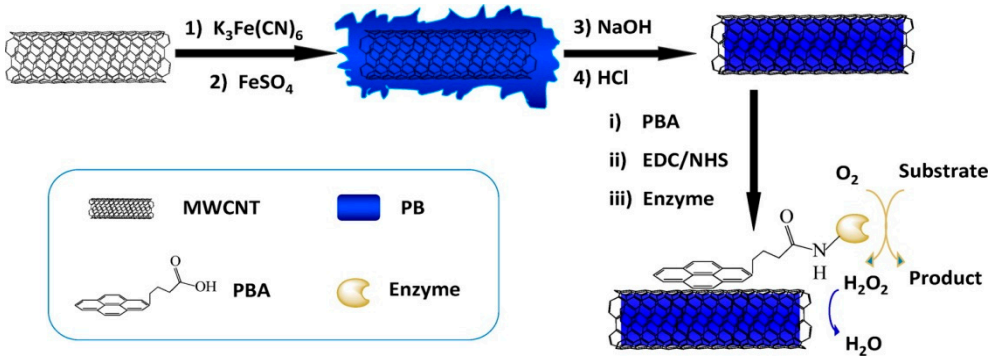

Figure 11. Scheme of synthesis of Enzyme-PBA/MWCNTs-PB_{in} for Biosensing. Reprinted with permission from reference [55]. Copyright (2012) American Chemical Society.

In light of the illustrated examples, it is clear that MWCNTs are the main nanoreactors used in the field. They provide a confined space big enough for nanoparticles encapsulation and for the diffusion of the products. In spite of the different types MWCNTs, this issue is generally disregarded in most cases. Zheng et al. studied the hydrogenation of dimethyl oxalate with Ag NPs confined within MWCNTs [29]. They reported a moderate increase of catalytic activity only at elevated liquid hourly space velocity when the NPs are encapsulated. This was surprising as Ag encapsulated form thin nanowires. A decrease of the catalytic activity was expected since endohedral NPs grew forming nanowires. Nanowires blocking MWCNTs channels would limit the transport diffusion. The authors brought to the scene the importance of MWCNTs type and compared the catalytic activity of Ag nanowires inside herringbone- or parallel-MWCNTs. Outstandingly, experiment with a reference material with adsorbed Cu nanoparticles confirmed activated-hydrogen migration through the graphitic planes of herringbone-MWCNTs. Contrarily, active species could not migrate through parallel-MWCNTs with a noticeable reduction of catalytic activity.

The use of thin double-walled CNTs (DWCNTs) and SWCNTs in this area is much less explored. Metal NPs would benefit from thinner internal diameter as this would limit the NPs size, enhancing activity. However, the restricted space (i.e., 0.5–2 nm diameter) may be detrimental for product diffusion as recently reported [62]. The authors reported a complete study of the confinement effect on Ru NPs towards the hydrogenation of alkenes. To do so, a full set of catalysts was prepared including SWCNTs decorated with Ru NPs both encapsulated and adsorbed, as well as graphene nanofibers (GNFs) also with both configurations. First experiments with standard laboratory equipment showed only a 10% norbonene reduction likely due to the limited internalization of reactants inside CNTs. The switch from cyclooctane as the solvent to supercritical CO_2 resulted in an increase of the yield up to 90%. As a comparison material, SWCNTs channels were elegantly blocked by fullerene encapsulation before Ru NPs deposition, in order to allow exclusive outer deposition, and the catalyst with this configuration afforded only 12% conversion, demonstrating the dramatic improvement of catalytic activity thanks to confinement. Comparison of norbonene and more bulky benzonorbonene reduction reflects the transport limitations within such small nanoreactors. Bigger GNFs with analogous Ru NPs appeared to have higher turnover numbers. Once again, confinement can be positive or negative with respect to the specific catalysis. In this case, there is a well-known positive confinement effect in GNFs and SWCNTs, yet the transport limitations are much smaller in GNFs, which made them a better candidate for further development.

6. Magnetic–Reaction Type IV

In some cases, the confined metal species turns out to be magnetic, making possible to capitalize on a simple recovery of the post-catalysis material [63]. For instance, Fe-filled CNTs (where the Fe species is magnetic) are relatively common examples. The presence of Fe may come very useful both in the material synthesis and during the recovery step, allowing a maximum recovery of the catalyst with a small energy input. Generally speaking, the use of magnetic NPs in heterogeneous catalysis represents a hot topic in research nowadays [64,65]. Very recently, our group reported the synthesis of nanohybrids made of covalently functionalized, Fe-filled MWCNTs covered with an inorganic layer of TiO_2 (or CeO_2) containing Pd NPs homogeneously distributed along the inorganic phase as evidenced by TEM-EDX imaging [66]. In this specific work, the inner magnetic phase was exploited for a double scope. In fact, after the hydrolysis of the metal oxide precursors, we systematically compared the advantages of magnetic purification against the classical, less selective filtration method. TEM imaging showed the presence of large inorganic agglomerates in the sample prepared by filtration, while ad-mixtures of the oxide were not observed in the samples magnetically purified. In other words, through confining magnetic Fe phases inside CNTs we were able to shepherd the individual inorganic-carbon hybrids while discarding isolated metal oxides. This has direct implication in the photocatalytic H_2 production, which was doubled for the more homogeneous sample, calling once again for the positive contribution of CNTs. Eventually, a NdFeB magnet was used to recover the photocatalyst, which was reused up to three times without a significant activity decrease (Figure 12).

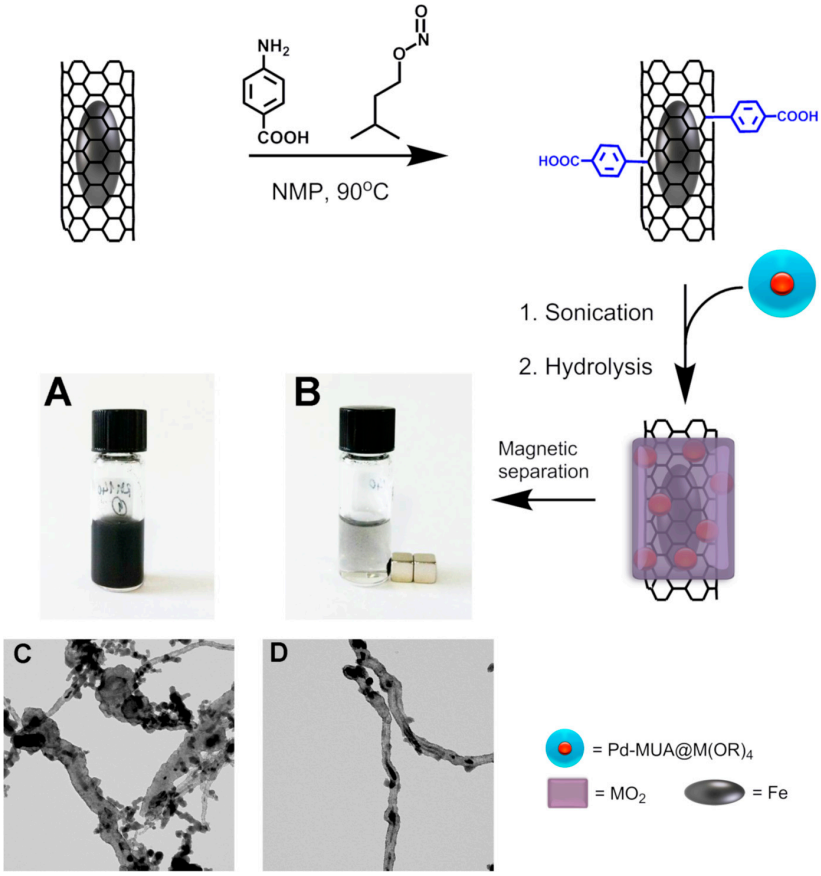

Figure 12. Graphic representation of the functionalization, hybridization, magnetic purification plus TEM characterization of Fe-filled CNTs covered with Pd and TiO_2 nanoparticles. (**A**) Photo of the dispersion of the nanohybrid in ethanol; (**B**) photo after magnetic separation from the dispersion; (**C**) TEM image of the nanohybrid recovered by filtration compared with (**D**) TEM image of the nanohybrid recovered after magnetic shepherding. Reprinted with permissions from reference [64]. Copyright Elsevier.

A similar approach was used in the work by Goh et al. for magnetically recycling CNTs-enzyme conjugate for up to 10 cycles of starch hydrolysis [66]. This reflects the versatility of CNTs that can accommodate materials from different nature (e.g., metal oxides or biomolecules) depending on the final application. In this case, the Mohr's salt (i.e., ammonium iron [II] sulfate) was used as Fe precursor to grow Fe_3O_4 NPs inside CNTs following a previuosly reported protocol protocol by Li et al. [67]. Differently, no magnetic purification was carried out as the activity of non-magnetic and magnetic samples were studied. The authors assessed also the effect of the nature of CNT-enzyme binding (i.e., covalent or noncovalent) and the stability of the hybrids under different storage conditions shedding light towards the deeper understanding of the topic. Interestingly, the lower enzymatic activity of the magnetic conjugates is paid back by the facile recovery. Overall, the amount of immobilized enzyme necessary to hydrolyse certain amount of starch is 8 times lower than the amount of free enzyme.

7. Traditional Catalysts–Reaction Type V

In the type V reaction, the metal NPs are completely encapsulated within closed-CNTs but the chemical conversion takes place outside CNTs. Then, the only possible effect of confinement must be related to the electronic communication between the inner component and the outer surface of the CNTs. Typically, this type of catalysts are employed in electrocatalytic applications, including development of fuel cells, sensors and batteries. These catalysts are far more stable and can be used under harsh reaction conditions. A proof was recently reported by Deng et al. on their work on ORR using 'pod-like' CNTs with Fe NPs inside [68]. During the synthesis, the materials needs to be refluxed in 25% HCl to remove the residual NPs, yet the unique structure of the so-called Pod-Fe remained unaltered and no signs of Fe oxidation were detected. Catalytic tests in H_2-O_2 single fuel cells afforded a voltage of 0.34 V at a current of 0.10 A cm^{-2} with only a 8% decrease in more than 200 h. Incorporation of N-doping atoms on the carbon graphitic network boosts the catalytic activity up to 60% more than the performance with Pt/C at the cathode where the oxygen reduction (ORR) occurs. Moreover, the catalyst appeared to be stable in the presence of common catalyst's poisons such as SO_2, or CN^- that easily coordinates Fe (Figure 13).

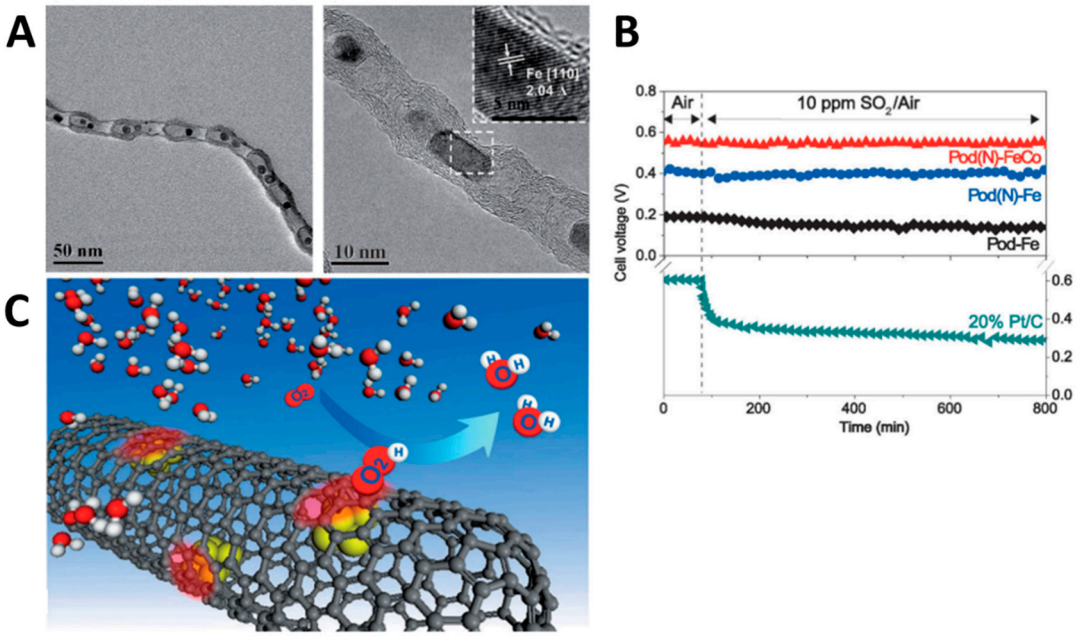

Figure 13. TEM images of 'pod-like' CNTs with encapsulated iron (**A**); (**B**) cell-voltage durability in air and in the presence of SO_2; and (**C**) graphical representation of the catalytic reaction. Adapted with permissions from reference [66]. Copyright Wiley and Sons.

Computational modelling of the hybrids revealed that CNTs work function decreases upon Fe encapsulation. This was confirmed by low-energy electron microscopy. As expected, the decrease of the work function resulted in an increase of reactivity. Oxidation of Pod-Fe occurred preferentially in the vicinity of Fe particles, which was oxidized after the decomposition of the carbon shield. In line, our team exploited a similar hybrid (i.e., Fe-filled MWCNTs) for the electrochemical ORR and hydrogen evolution reactions at physiological pH, after covalent functionalization of the CNTs with benzoic acid units [17]. In our view, together with a decrease of the MWCNTs work function, there are other effects such as the higher affinity for the substrate due to the grafted functional groups and the cross-linking defects, which boost the electronic communication between different components. Analogues effect are in general described for this kind of hybrid materials. Hierarchical materials made of N doped CNTs, rGO and Co nanoparticles afforded electrocatalytic hydrogen production very close to commercial 20% Pt supported on C [33]. The catalytic activity in acid media was preserved after 100 h, confirming once again the protective role of the carbon layer. Such complex material was split in simpler fragments to study the hydrogen adsorption. Apart from naked Co that interacts strongly with hydrogen, the interaction with Co@N-C was much favoured with respect to the integration with the other components (i.e., graphene, N-doped graphene or Co encapsulated in graphene). The overall performance of the material was explained by the synergy between large surface area and adequate porous structure, the efficient hydrogen adsorption and charge transfer between the graphitic surface and the metal.

Hydrazine direct fuel cells are emerging as an intriguing alternative to other more traditional fuel cells [69]. Recently, CNTs filled with Ni-Fe alloys exhibited superior catalytic activity towards hydrazine oxidation than reference catalysts with different configurations. The hybrid catalyst was accessed by methylbenzene-oriented constant current electrodeposition [70].

8. Conclusions and Outlook

This review has highlighted some of the recent developments in CNT catalysis by exploiting the inner cavity of the tubular carbon phase that results in the emergence of fascinating catalytic properties for several chemical conversions. There are a number of advantages that such a strategy allows, and the field is expected to produce new brilliant breakthroughs thanks to the progress in CNT-related synthetic knowledge and characterization techniques. The nanometric confinement effect has the potential to completely alter the catalytic features, in many cases with positive effects. For some time, filled CNTs or use of the inner cavity as a nanoreactor have been overlooked due to the difficulty in selectively confining foreign species within the tubes. However, this limitation no longer exists and now is the time to generate new groundbreaking research on this topic. In turn, this would cause a renaissance of catalysts based on CNTs, which has been partially overshadowed by the rise of graphene as a preferred carbon component of late. Multiple assets can be gained from nano-confinement, so future work should focus on the benefits of confinement in relation to the specific reaction, which may improve upon simple enhancements of intrinsic catalytic activity.

Acknowledgments: The University of Trieste is kindly acknowledged for funding.

Conflicts of Interest: The authors declare no conflict of interest.

References

1. Tasis, D.; Tagmatarchis, N.; Bianco, A.; Prato, M. Chemistry of carbon nanotubes. *Chem. Rev.* **2006**, *106*, 1105–1136. [CrossRef] [PubMed]
2. Melchionna, M.; Marchesan, S.; Marchesan, S.; Prato, M.; Fornasiero, P. Carbon Nanotubes and Catalysis: The many facets of a successful marriage. *Catal. Sci. Technol.* **2015**, *5*, 3859–3875. [CrossRef]
3. Geim, A.K.; Novoselov, S. The rise of graphene. *Nat. Mater.* **2007**, *6*, 183–191. [CrossRef] [PubMed]
4. Melchionna, M.; Prato, M. Functionalizing carbon canotubes: Cn indispensible step towards applications. *ECS J. Solid State Sci. Technol.* **2013**, *2*, M3040–M3045. [CrossRef]

5. Chen, Z.; Thiel, W.; Hirsch, A. Reactivity of the convex and concave surfaces of single-walled carbon nanotubes (SWCNTs) towards addition reactions: rependence on the carbon-atom pyramidalization. *ChemPhysChem* **2003**, *4*, 93–97. [CrossRef] [PubMed]
6. Pan, X.; Bao, X. The effects of confinement inside carbon. *Acc. Chem. Res.* **2011**, *44*, 553–562. [CrossRef] [PubMed]
7. Kondratyuk, P.; Yates, J.T. Molecular views of physical adsorption inside and outside of single-wall carbon nanotubes. *Acc. Chem. Res.* **2007**, *40*, 995–1004. [CrossRef]
8. Guan, J.; Pan, X.; Liu, X.; Bao, X.J. Syngas segregation induced by confinement in carbon nanotubes: A combined first-principles and montecarlo sudy. *Phys. Chem. C* **2009**, *113*, 21687–21692. [CrossRef]
9. Kim, H.; Sigmund, W.J. Iron nanoparticles in carbon nanotubes at various temperatures. *Cryst. Growth* **2005**, *276*, 594–605. [CrossRef]
10. Khabashesku, V.N.; Billups, W.E.; Margrave, J.L. Fluorination of single-wall carbon nanotubes and subsequent derivatization reactions. *Acc. Chem. Res.* **2002**, *35*, 1087–1095. [CrossRef]
11. Khlobystov, A.N.; Britz, D.A.; Briggs, G.A.D. Molecules in carbon nanotubes. *Acc. Chem. Res.* **2005**, *38*, 901–909. [CrossRef] [PubMed]
12. Khlobystov, A.N. Carbon nanotubes: From nanotest tube to nano-reactor. *ACS Nano* **2011**, *5*, 9306–9312. [CrossRef] [PubMed]
13. Zhang, J.; Müller, J.O.; Zheng, W.; Wang, D.; Su, D.; Schlögl, R. Individual Fe-Co allory nanoparticles on carbon nanotubes: Structural and catalytic properties. *Nano Lett.* **2008**, *8*, 2738–2743. [CrossRef] [PubMed]
14. Pan, X.; Fan, Z.; Chen, W.; Ding, Y.; Luo, H.; Bao, X. Enhanced ethanol production inside carbon-nanotube reactors containing catalytic particles. *Nat. Mater.* **2007**, *6*, 507–511. [CrossRef] [PubMed]
15. Tsang, S.C.; Chen, Y.K.; Harris, P.J.F.; Green, M.L.H. A simple chemical method of opening and filling carbon nanotubes. *Nature* **1994**, *372*, 159–162. [CrossRef]
16. Talyzin, A.V.; Anoshkin, I.V.; Nasibulin, A.G.; Krasheninnikov, A.V.; Nieminen, R.M.; Jiang, H.; Kauppinen, E.I. Synthesis of graphene nanoribbons encapsulated in single-wall carbon nanotubes. *Nano Lett.* **2011**, *11*, 4352–4356. [CrossRef] [PubMed]
17. Bracamonte, M.V.; Melchionna, M.; Stopin, A.; Giulani, A.; Tavagnacco, C.; Garcia, Y.; Fornasiero, P.; Bonifazi, D.; Prato, M. Carboxylated, Fe-filled multiwalled carbon nanotube as versatile catalysts for O_2 reduction and H_2 evolution reactions at physiological pH. *Chem. A Eur. J.* **2015**, *21*, 12769–12777. [CrossRef]
18. Sengupta, J.; Jacob, C.J. The effect of Fe and Ni catalysts on the growth of multiwalled carbon nanotubes using chemical vapor deposition. *Nanopart. Res.* **2010**, *12*, 457–465. [CrossRef]
19. Suryanto, B.H.R.; Fang, T.; Cheong, S.; Tilley, R.D.; Zhao, C. From the inside-out: Leached metal impurities in multiwall carbon nanotubes for purification or electrocatalysis. *J. Mater. Chem. A* **2018**, *6*, 4686–4694. [CrossRef]
20. Baaziz, W.; Liu, X.; Florea, I.; Begin-Colin, S.; Pichon, B.P.; Ulhaq, C.; Ersen, O.; Soria-Sánchez, M.; Zafeiratos, S.; Janowska, I.; et al. Carbon nanotube channels selectivity filled with monodispersed $Fe_{3-x}O_4$ nanoparticles. *J. Mater. Chem. A* **2013**, *1*, 13853–13861. [CrossRef]
21. Baaziz, W.; Begin-Colin, S.; Pichon, B.P.; Florea, I.; Ersen, O.; Zafeiratos, S.; Barbosa, R.; Begin, D.; Pham-Huu, C. High-density monodispersed cobalt nanoparticles filled into multiwalled carbon nanotubes. *Chem. Mater.* **2012**, *24*, 1549–1551. [CrossRef]
22. Castillejos, E.; Debouttière, P.J.; Roiban, L.; Solhy, A.; Martinez, V.; Kihn, Y.; Ersen, O.; Philippot, K.; Chaudret, B.; Serp, P. An efficient strategy to drive nanoparticles into carbon nanotubes and the remarkable effect of confinement on their catalytic performance. *Angew. Chem. Int. Ed.* **2009**, *48*, 2529–2533. [CrossRef] [PubMed]
23. Ersen, O.; Werckmann, J.; Houllé, M.; Ledoux, M.J.; Pham-Huu, C. 3D electron microscopy study of metal particles inside multiwalled carbon nanotubes. *Nano Lett.* **2007**, *7*, 1898–1907. [CrossRef] [PubMed]
24. Guan, L.; Shi, Z.; Li, M.; Gu, Z. Ferronce-filled single-walled carbon nanotubes. *Carbon* **2005**, *43*, 2780–2785. [CrossRef]
25. Yanagi, K.; Iakoubovskii, K.; Matsui, H.; Matsuzaki, H.; Okamoto, H.; Miyata, Y.; Maniwa, Y.; Kazaoui, S.; Minami, N.; Kataura, H. Photosensitive function of encapsulated dye in carbon nanotubes. *J. Am. Chem. Soc.* **2007**, *129*, 4992–4997. [CrossRef] [PubMed]
26. Yanagi, B.K.; Miyata, Y.; Kataura, H. Highly stabilized β-carotene in carbon nanotubes. *Adv. Mater.* **2006**, *18*, 437–441. [CrossRef]

27. Nieto-Ortega, B.; Villalva, J.; Vera-Hidalgo, M.; Ruiz-González, L.; Burzurí, E.; Pérez, E.M. Band-gap opening in metallic single-walled carbon nanotubes by encapsulation of an organic salt. *Angew. Chem. Int. Ed.* **2017**, *56*, 12240–12244. [CrossRef] [PubMed]
28. Kierkowicz, M.; González-Domínguez, J.M.; Pach, E.; Sandoval, S.; Ballesteros, B.; Da Ros, T.; Tobias, G. Filling single-walled carbon nanotubes with lutetium chloride: A sustainable production of nanocapsules free of nonencapsulated material. *ACS Sustain. Chem. Eng.* **2017**, *5*, 2501–2508. [CrossRef]
29. Zheng, J.; Duan, X.; Lin, H.; Gu, Z.; Fang, H.; Li, J.; Yuan, Y. Silver nanoparticles confined in carbon nanotubes: On the understanding of the confinement effect and promotional catalysis for the selective hydrogenation of dimethyl oxalate. *Nanoscale* **2016**, *8*, 5959–5967. [CrossRef]
30. Accolti, L.D.; Gajewska, A.; Kierkowicz, M.; Martincic, M.; Nacci, N.; Sandoval, S.; Tobias, G.; Da Ros, T.; Fusco, C. Epoxidation of carbon nanocapsules: Decoration of single-walled carbon nanotubes filled with metal halides. *Nanomaterials* **2018**, *8*, 137. [CrossRef]
31. Marega, R.; De Leo, F.; Pineux, F.; Sgrignani, J.; Magistrato, A.; Naik, A.D.; Garcia, Y.; Flamant, L.; Michiels, C.; Bonifazi, D. Functionalized Fe-filled multiwalled carbon nanotubes as multifunctional scaffolds for magnetization of cancer cells. *Adv. Funct. Mater.* **2013**, *23*, 3173–3184. [CrossRef]
32. Bahr, J.L.; Yang, J.; Kosynkin, D.V.; Bronikowski, M.J.; Smalley, R.E.; Tour, J. Functionalization of carbon nanotubes by electrochemical reduction of aryl diazonium salts: A bucky paper electrode. *J. Am. Chem. Soc.* **2001**, *123*, 6536–6542. [CrossRef] [PubMed]
33. Chen, Z.; Wu, R.; Liu, Y.; Ha, Y.; Guo, Y.; Sun, D.; Liu, M. Ultrafine Co nanoparticles encapsulated in carbon-nanotubes-grafted graphene sheets as advanced electrocatalysts for the hydrogen evolution reaction. *Adv. Mater.* **2018**, *30*, 1802011. [CrossRef] [PubMed]
34. Byl, O.; Liu, J.; Wang, Y.; Yim, W.; Johnson, J.K.; Yates, J.T.; Chemie, A.; Carl, V.; Uni, O.; Str, C.-V.; et al. Unusual hydrogen bonding in water-filled carbon nanotubes. *J. Am. Chem. Soc.* **2006**, *128*, 12090–12097. [CrossRef] [PubMed]
35. Miners, S.A.; Rance, G.A.; Khlobystov, A.N. Chemical reactions confined within carbon nanotubes. *Chem. Soc. Rev.* **2016**, *45*, 4727–4746. [CrossRef] [PubMed]
36. Miners, S.A.; Rance, G.A.; Khlobystov, A.N. Regioselective control of aromatic halogenation reactions in carbon nanotube nanoreactors. *Chem. Commun.* **2013**, *49*, 5586–5588.
37. Marforio, T.D.; Bottoni, A.; Giacinto, P.; Zerbetto, F.; Calvaresi, M. Aromatic bromination of N-phenylacetamide inside CNTs. Are CNTs real nanoreactors controlling regioselectivity and kinetics? A QM/MM investigation. *J. Phys. Chem. C* **2017**, *121*, 27674–27682. [CrossRef]
38. Talyzin, A.V.; Luzan, S.M.; Leifer, K.; Akhtar, S.; Fetzer, J.; Cataldo, F.; Tsybin, Y.O.; Tai, C.W.; Dzwilewski, A.; Moons, E. Coronen fusion by heat treatment: Road to nanographene. *J. Phys. Chem. C* **2011**, *115*, 13207–13214. [CrossRef]
39. Chuvilin, A.; Bichoutskaia, E.; Gimenez-Lopez, M.C.; Chamberlain, T.W.; Rance, G.A.; Kuganathan, N.; Biskupek, J.; Kaiser, U.; Khlobystov, A.N. Self-assembly of a sulphur-terminated graphene nanoribbon within a single-walled carbon nanotube. *Nat. Mater.* **2011**, *10*, 687–692. [CrossRef] [PubMed]
40. Chamberlain, T.W.; Biskupek, J.; Rance, G.A.; Chuvilin, A.; Alexander, T.J.; Bichoutskaia, E.; Kaiser, U.; Khlobystov, A.N. Size, structure, and helical twist of graphene nanoribbons controlled by confinement in carbon nanotubes. *ACS Nano* **2012**, *6*, 3943–3953. [CrossRef] [PubMed]
41. Nakamura, E.; Koshino, M.; Saito, T.; Niimi, Y.; Suenaga, K.; Matsuo, Y. Electron microscopy imaging of a single group 8 metal atom catalyzing C-C bond reorganization of fullerenes. *J. Am. Chem. Soc.* **2011**, *133*, 14151–14153. [CrossRef] [PubMed]
42. Koshino, M.; Niimi, Y.; Nakamura, E.; Kataura, H.; Okazaki, T.; Suenaga, K.; Iijima, S. Analysis of the reactivity of fullerene dimerization reactions at the atomic level. *Nat. Chem.* **2010**, *2*, 117–124. [CrossRef] [PubMed]
43. Nakanishi, Y.; Omachi, H.; Fokina, N.A.; Schreiner, P.R.; Kitaura, R.; Dahl, J.E.P.; Carlson, R.M.K.; Shinohara, H. Template synthesis of linear-chain nanodiamonds inside carbon nanotubes from bridgehead-halogenated diamantane precursors. *Angew. Chem. Int. Ed.* **2015**, *54*, 10802–10806. [CrossRef] [PubMed]
44. Miyaura, K.; Miyata, Y.; Thendie, B.; Yanagi, K.; Kitaura, R.; Yamamoto, Y.; Arai, S.; Kataura, H.; Shinohara, H. Extended-conjugation π-electron systems in carbon nanotubes. *Sci. Rep.* **2018**, *8*, 8098. [CrossRef] [PubMed]

45. Li, X.; Zhang, L.; Tan, R.P.; Fazzini, P.F.; Hungria, T.; Durand, J.; Lachaize, S.; Sun, W.H.; Respaud, M.; Soulantica, K.; et al. Isoprene polymerization on iron nanoparticles confined in carbon nanotubes. *Chem. A Eur. J.* **2015**, *21*, 17437–17444. [CrossRef] [PubMed]
46. Cabana, L.; Ballesteros, B.; Batista, E.; Magén, C.; Arenal, R.; Oró-solé, J.; Rurali, R.; Tobias, G. Synthesis of PbI_2 single-layered inorganic nanotubes encapsulated within carbon nanotubes. *Adv. Mater.* **2014**, *26*, 2016–2021. [CrossRef] [PubMed]
47. Kreizman, R.; Enyashin, A.N.; Deepak, F.L.; Albu-Yaron, A.; Popovitz-Biro, R.; Seifert, G.; Tenne, R. Synthesis of core-shell inorganic nanoparticles. *Adv. Funct. Mater.* **2010**, *20*, 2459–2468. [CrossRef]
48. Kreizman, R.; Hong, S.Y.; Sloan, J.; Popovitz-Biro, R.; Albu-Yaron, A.; Tobias, G.; Ballesteros, B.; Davis, B.G.; Green, M.L.H.; Tenne, R. Core-shell PbI_2@WS_2 inorganic nanotubes from capilarry wetting. *Angew. Chem. Int. Ed.* **2009**, *48*, 1230–1233. [CrossRef]
49. Ashokkumar, A.E.; Enyashin, A.N.; Deepak, F.L. Single walled BiI3 nanotubes encapsulated within carbon nanotubes. *Sci. Rep.* **2018**, *8*, 2–9. [CrossRef]
50. Fedoseeva, Y.V.; Orekhov, A.S.; Chekhova, G.N.; Koroteev, V.O.; Kanygin, M.A.; Senkovskiy, B.V.; Chuvilin, A.; Pontiroli, D.; Riccò, M.; Bulusheva, L.G.; et al. Single-walled carbon nanotube reactor for redox transformation of mercury dichloride. *ACS Nano* **2017**, *11*, 8643–8649. [CrossRef]
51. Cox, M.; El-Shafey, E.; Pichugin, A.A.; Appleton, Q.J. Removal of mercury (II) from aqueous solution on a carbonaceous sorbent prepared from flax shive. *Chem. Technol. Biotechnol.* **2000**, *75*, 427–435. [CrossRef]
52. Castillejos, E.; Chico, R.; Bacsa, R.; Coco, S.; Espinet, P.; Pérez-Cadenas, M.; Guerrero-Ruiz, A.; Rodríguez-Ramos, I.; Serp, P. Selective deposition of gold nanoparticles on or inside carbon nanotubes and their catalytic activity for preferencial oxidation of CO. *Eur. J. Inorg. Chem.* **2010**, *2010*, 5096–5102. [CrossRef]
53. Liu, J.; Liu, R.; Li, H.; Kong, W.; Huang, H.; Liu, Y.; Kang, Z. Au nanoparticles in carbon nanotubes with high photocatalytic activity for hydrocarbon selective oxidation. *Dalt. Trans.* **2014**, *43*, 12982–12988. [CrossRef] [PubMed]
54. Cui, X.; Wang, Y.; Jiang, G.; Zhao, Z.; Xu, C.; Duan, A.; Liu, J.; Wei, Y.; Bai, W. The encapsulation of CdS in carbon nanotubes for stable and efficient photocatalysis. *J. Mater. Chem. A* **2014**, *2*, 20939–20946. [CrossRef]
55. Chen, W.; Fan, Z.; Zhang, B.; Ma, G.; Takanabe, K.; Zhang, X.; Lai, Z. Enhanced visible-light activity of titania via confinement inside carbon nanotubes. *J. Am. Chem. Soc.* **2011**, *133*, 14896–14899. [CrossRef] [PubMed]
56. Liu, H.; Zhang, L.; Wang, N.; Su, D.S. Palladium nanoparticles embedded in the inner surfaces of carbon nanotubes: Synthesis, catalytic activity, and sinter resistance. *Angew. Chem. Int. Ed.* **2014**, *53*, 12634–12638. [CrossRef] [PubMed]
57. Chen, W.; Fan, Z.; Pan, X.; Bao, X. Reactions over catalysts confined in carbon nanotubes. *J. Am. Chem. Soc.* **2008**, *130*, 9414–9419. [CrossRef]
58. Guo, S.; Pan, X.; Gao, H.; Yang, Z.; Zhao, J.; Bao, X. Probing the electronic effect of carbon nanotubes in catalysis: NH_3 synthesis with Ru nanoparticles. *Chem. A Eur. J.* **2010**, *16*, 5379–5384. [CrossRef]
59. Zheng, W.; Zhang, J.; Zhu, B.; Blume, R.; Zhang, Y.; Schlichte, K.; Schlçgl, R.; Schöth, F.; Su, D.S. Structure-function correlations for Ru/CNT in the catalytic decomposition of ammonia. *ChemSusChem* **2010**, *3*, 226–230. [CrossRef]
60. Wang, T.; Fu, Y.; Chai, L.; Chao, L.; Bu, L.; Meng, Y.; Chen, C.; Ma, M.; Xie, Q.; Yao, S. Filling carbon nanotubes with prussian blue nanoparticles of high peroxidase-like catalytic activity for colorimetric chemo- and biosensing. *Chem. A Eur. J.* **2014**, *20*, 2623–2630. [CrossRef]
61. Wang, T.; Fu, Y.; Bu, L.; Qin, C.; Meng, Y.; Chen, C.; Ma, M.; Xie, Q.; Yao, S. Facile synthesis of prussian blue-filled multiwalled carbon nanotubes nanocomposites: exploring filling/electrochemistry/mass-transfer in nanochannels and cooperative biosensing mode. *J. Phys. Chem. C* **2012**, *116*, 20908–20917. [CrossRef]
62. Aygun, M.; Stoppiello, C.T.; Lebedeva, M.A.; Smith, E.F.; del C. Giménez-López, M.; Khlobystov, A.N. Comparison of alkene hydrogenation in carbon nanoreactors of different diameters: Probing the effect of nanoscale confinement on ruthenium nanoparticle catalysis. *J. Mater. Chem. A* **2017**, *117*, 21467–21477. [CrossRef]
63. Rossella, F.; Mozzati, M.C.; Bordonali, L.; Lascialfari, A.; Soldano, C.; Ortolani, L.; Bellani, V. Nanostructured magnetic metamaterials based on metall-filled carbon nanotubes. *Carbon* **2016**, *96*, 720–728. [CrossRef]
64. Gawande, M.B.; Luque, R.; Zboril, R. The rise of magnetically recyclable nanocatalysts. *ChemCatChem* **2014**, *6*, 3312–3313. [CrossRef]

65. Shylesh, S.; Schünemann, V.; Thiel, W.R. Magnetically separable nanocatalysts: Bridges between homogeneous and heterogeneous catalysis. *Angew. Chem. Int. Ed.* **2010**, *49*, 3428–3459. [CrossRef] [PubMed]
66. Melchionna, M.; Beltram, A.; Stopin, A.; Montini, T.; Lodge, R.W.; Khlobystov, A.N.; Bonifazi, D.; Prato, M.; Fornasiero, P. Magnetic shepherding of nanocatalysts through hierarchically-assembled Fe-filled CNTs. *Appl. Catal. B Environ.* **2018**, *227*, 356–365. [CrossRef]
67. Li, J.H.; Hong, R.Y.; Luo, G.H.; Zheng, Y.; Li, H.Z.; Wei, D.G. An easy approach to encapsulating Fe_3O_4 nanoparticles in multiwalled carbon nanotubes. *New Carbon Mater.* **2010**, *25*, 192–198. [CrossRef]
68. Deng, D.; Yu, L.; Chen, X.; Wang, G.; Jin, L.; Pan, X.; Deng, J.; Sun, G.; Bao, X. Iron encapsulated within pod-like carbon nanotubes for oxygen reduction reaction. *Angew. Chem. Int. Ed.* **2013**, *52*, 371–375. [CrossRef]
69. Zhang, T.; Asefa, T. Heteroatom-doped carbon materials for hydrazineoxidation. *Adv. Mater.* **2018**. [CrossRef]
70. Wang, J.; Dong, Z.; Huang, J.; Li, J.; Jin, X.; Niu, J.; Sun, J.; Jin, J.; Ma, J. Filling carbon nanotubes with Ni-Fe alloys via methylbenzene-oriented constant current electrodeposition for hydrazine electrocatalysis. *Appl. Surf. Sci.* **2013**, *270*, 128–132. [CrossRef]